Palaeogeography, Palaeoclimatology, Palaeoecology 285 (2010) 66–73

Contents lists available at ScienceDirect

Palaeogeography, Palaeoclimatology, Palaeoecology

journal homepage: www.elsevier.com/locate/palaeo

Late Miocene paleoenvironmental changes in North Africa and the Mediterranean recorded by geochemical proxies (Monte Gibliscemi section, Sicily)

C.M. Köhler [a,*], D. Heslop [b], W. Krijgsman [c], M.J. Dekkers [c]

[a] Department of Geology and Petroleum Geology, University of Aberdeen, Meston Building, Aberdeen, AB24 3UE, United Kingdom
[b] University of Bremen, FB Geowissenschaften, Postfach 330440, Bremen, Germany
[c] Paleomagnetic Laboratory 'Fort Hoofddijk', University of Utrecht, Budapestlaan 17, 3584 CD Utrecht, The Netherlands

ARTICLE INFO

Article history:
Received 29 September 2008
Received in revised form 9 October 2009
Accepted 18 October 2009
Available online 24 October 2009

Keywords:
Geochemical proxy parameters
Palaeoclimate
Eastern Mediterranean
Late Miocene
Biosiliceous production

ABSTRACT

The astronomically tuned marls of the Monte Gibliscemi section, Sicily, constitute an archive to trace the late Miocene palaeoenvironmental conditions (~9.7–7.0 Ma) in North Africa. Here we have utilised carbonate content and Al-normalised geochemical proxies to trace changes in terrigenous source area and bottom-water ventilation. The terrigenous input into the section is dominated by North African river systems draining into the Eastern Mediterranean. The proxy parameters indicate that the palaeoenvironmental conditions in North Africa were humid from 9.5 Ma onward with high fluvial input to the Mediterranean. Increases in the Si/Al and Mg/Al ratios occurred from 8.4 to 8.2 Ma and from 8.05 to 7.75 Ma, with maximum values similar to those of Messinian diatomites. These peaks indicate conditions of enhanced biosiliceous productivity and the presence of authigenic clay formation. Sluggish water circulation in the Mediterranean during those times is inferred from the Mn/Al and V/Al behaviour. Late Miocene changes of the Betic (southern Spain) and Rifian (Morocco) Mediterranean–Atlantic gateways are interpreted as the driving force for the changes in water circulation and the transgression associated with the opening of the Rifian corridor is interpreted to occur at 7.8 Ma.

1. Introduction

The late Miocene North African climate is generally considered to have been much more humid than today (Ruddiman et al., 1989; Griffin, 2002; Lihoreau et al., 2006; Gladstone et al., 2007; Köhler et al., 2008). Humid palaeoenvironmental conditions support a denser vegetation cover binding the soil and reducing dust production (Middleton, 1985; Larrasoaña et al., 2003a). Higher precipitation, especially in North Central Africa, also feeds the rivers that drained into the central and eastern Mediterranean Sea (e.g. Burke and Wells, 1989; Griffin, 2002; Gladstone et al., 2007), leaving records of North African climate change in its sediments. The elements Si, Ti, Mg and Al are associated with specific mineral phases and weathering conditions, and may thus indicate changes in North African palaeoenvironment and dust production (Lourens et al., 2001; Larrasoaña et al., 2003a). African terrigenous supply can be traced by specific elemental ratios, e.g. Si/Al, Ti/Al and Mg/Al (e.g. Bergametti et al., 1989; Wehausen and Brumsack, 2000; Lourens et al., 2001).

Knowledge of the hydrological budget of the late Miocene is important for model calculations of salt precipitation during the Messinian Salinity Crisis, which currently relies on modern hydrological data (Benson et al., 1991; Flecker et al., 2002; Meijer and Krijgsman, 2005). It was shown by Meijer and Krijgsman (2005) that the degree of saturation required for salt precipitation depends on the freshwater input into the Eastern Mediterranean; therefore knowledge of the river runoffs becomes very important.

The palaeoceanographic evolution of the Mediterranean region during the Tortonian and early Messinian is marked by several well-defined paleoenvironmental changes (Hüsing et al., 2009). In a recent sediment provenance study, African source area changes during the late Miocene were reconstructed using geochemical and environmental magnetic proxies obtained from the astronomically dated Metochia sediment sequences of Gavdos Island in the Eastern Mediterranean (Köhler et al., 2008). Changes in the proxy records mainly took place between 8.4 and 8.2 Ma and suggested less aeolian dust input after 8.2 Ma and thus more humid conditions in North Africa. This picture is complicated however, because the Gavdos record is also modulated by changes in the Aegean source area due to concurrent regional tectonics (Köhler et al., in press).

Here, we aim to track and distinguish late Miocene climatic changes over North Africa in the sedimentary record of the Monte Gibliscemi section in southern Sicily using geochemical data. Monte Gibliscemi provides a suitable archive of astronomically dated marine sediments spanning the time period from 9.7 to 7 Ma (Krijgsman et al., 1995), thus covering the proposed time interval of inferred climate change. The section is located in the central Mediterranean

* Corresponding author. Tel.: +44 1224 27343; fax: +44 1224 277785.
E-mail address: ckoehler@uni-bremen.de (C.M. Köhler).

0031-0182/$ – see front matter © 2009 Elsevier B.V. All rights reserved.
doi:10.1016/j.palaeo.2009.10.025

basin close to the North African continent and far away from other continental source areas (Orszag-Sperber et al., 1993). Consequently, it is reasonable to anticipate that the African signal dominates the terrigenous input.

2. Materials and methods

2.1. Section, age model and samples

The Monte Gibliscemi section is located in southern Sicily (Fig. 1) and consists of subsections A and B (Krijgsman et al., 1995). The Monte Gibliscemi sediments were deposited under deep marine conditions of ~1200 m (Krijgsman et al., 1995; Kouwenhoven et al., 2003) and span the time interval 9.77–6.97 Ma, with a hiatus between 7.52 and 7.24 Ma (Hilgen et al., 1995; Krijgsman et al., 1995). The section has a characteristic cyclicity of alternating sapropels and homogeneous marls. A precise age model was constructed by (Hilgen et al., 1995) based on a combination of cyclo- and biostratigraphy. Individual sapropels were correlated with precession minima, small sapropel clusters to 100 kyr eccentricity maxima and large scale sapropel clusters to 400 kyr eccentricity maxima (Hilgen et al., 1995). The characteristic sapropel patterns were tuned to the 65°N summer insolation solution of Laskar. Here we use revised sapropel ages (Laskar et al., 2004), which cause an average 2.5 kyr shift to younger ages.

In the present study, only the homogeneous marls of the late Tortonian were investigated because they are less affected by diagenetic alterations than sapropels and are therefore more likely to provide a primary terrigenous signal. The marls represent the arid phase of the sapropel–marl cycle (e.g. van Os et al., 1994; Rossignol-Strick et al., 1998), making them a suitable archive of changes in North African palaeoenvironmental conditions. In total, 268 pristine marl samples from the original stratigraphic sample set of Krijgsman et al. (1995) were used, with three samples per marl bed giving an average temporal spacing of 0.009 Myr.

2.2. Bulk geochemical analysis

To determine the geochemical composition of the Monte Gibliscemi marls, X-ray fluorescence analysis (XRF) was performed on the planar surfaces of solid cylindrical samples (~4 g) using a Spectro Xepos energy dispersive polarization X-ray fluorescence analyzer. The measuring time was 300 s per sample. Accuracy and precision were checked using the internal marine standard Mag-1 (certified USGS marine sediment standard reference material) and duplicate measurements. Measurement errors are <5% for the elements Al, Ca, Si, Mg, Ti, Fe and Mn in this study; V has a higher error of ~20%.

The larger error of V is unfortunate but acceptable, because we compare only V peaks to peaks of Fe and Mn without trying to use its entire concentration range. The stable terrigenous element Al plays an important role in the geochemical interpretation because the abundances of other elements can be normalised against it to compensate for dilution effects (Wehausen and Brumsack, 1998; Schenau et al., 1999; Wehausen and Brumsack, 2000; Lourens et al., 2001; Larrasoaña et al., 2003a). The normalisation further enables comparison with other late Miocene geochemical studies (Köhler et al., 2008) and Pleistocene studies of the Eastern Mediterranean (e.g. Wehausen and Brumsack, 1998, 2000).

2.3. Clay mineralogy

Mineral identification using X-ray diffraction (XRD) was performed on a few selected samples using a *Philips X'Pert Pro* multipurpose diffractometer with a Cu tube and an automated divergence slit of 110° 2θ. Seven samples for the XRD analysis were picked on the basis of the geochemical and colour data (unpublished data). Approximately 4 g of finely ground bulk sediment (<20 μm particle size) was pressed into a pellet for the measurements using a Philips backloading system. The measurements were performed on a Philips X'Pert Pro multipurpose diffractometer equipped with a Cu tube (k″ 1.541, 45 kV, 40 mA), a fixed divergence slit of ″° 2θ, a 16 sample changer, a secondary monochromator and the X'Celerator detector system, as continuous scans from 3–85° 2θ with a calculated step size of 0.016° 2θ. Data were analysed using the Philips software X'Pert HighScore™ package, which provides a semi-quantitative abundance for each identified mineral. For a more detailed description of the method see Vogt et al. (2002).

3. Results

3.1. Geochemistry and sedimentation rate

Variations in sediment supply in the marls below the hiatus are traced by sedimentation rate and Al mass accumulation rate (MAR) (Peterson et al., 2000). The sedimentation rate at Monte Gibliscemi has its lowest values of ~2 cm/kyr in the older parts of the section. From 9.6 Ma onward values increase and remain high throughout the section, with maximum values of ~7.5 cm/kyr (Fig. 2). There are two drops at 8.5 Ma and 7.75 Ma, after which the sedimentation rate recovers again to its highest values (Fig. 2). The Al-MAR has its lowest

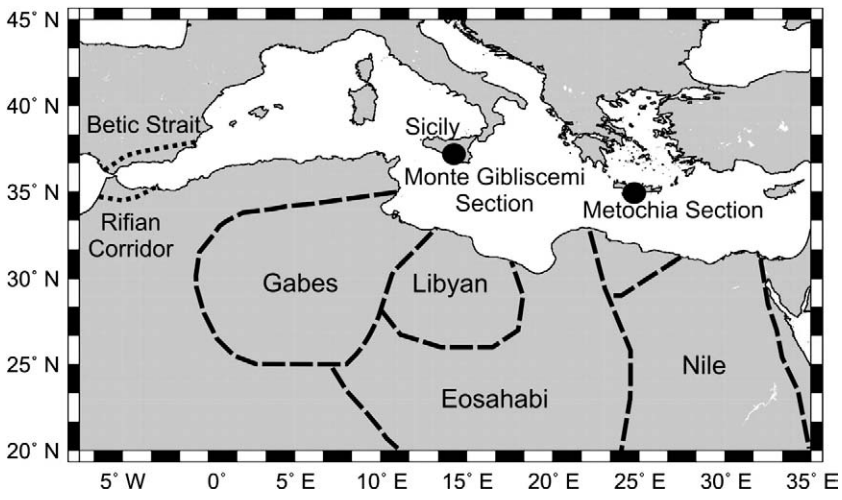

Fig. 1. Map of the Mediterranean Sea and North Africa. The locations of the studied sections are marked with circles. The approximate boundaries of the late Miocene river systems of North Africa are indicated with dashed lines (Griffin, 2002; Gladstone et al., 2007). The late Tortonian gateways connecting the Mediterranean Sea with the Atlantic Ocean are marked with black dotted lines (Krijgsman et al., 1999).

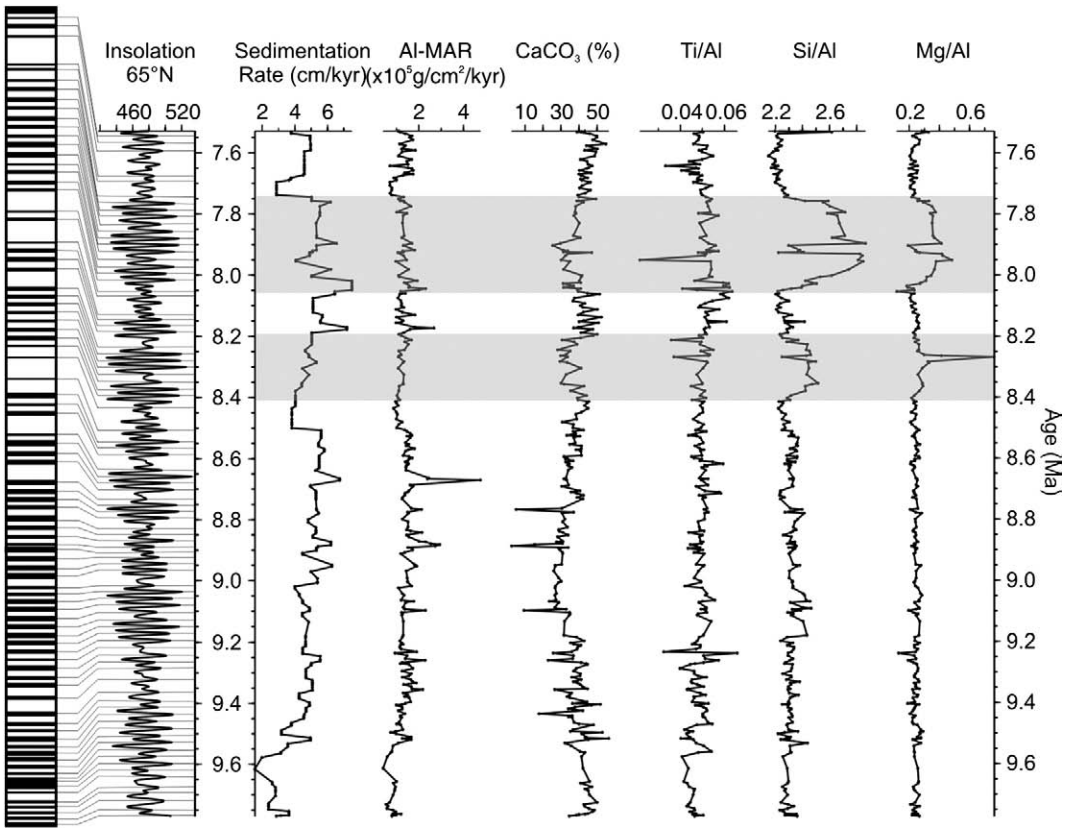

Fig. 2. Monte Gibliscemi section. Age profiles of the proxies discussed in the text, below the hiatus, and a stratigraphic column to show the marl–sapropel pattern of the Monte Gibliscemi section, where white = homogenous marls, black = sapropels; (taken from: Krijgsman et al., 1995). The grey bars indicate two intervals of enhanced Si/Al and Mg/Al ratios, when also ratios indicative of reduction in the bottom-water ventilation are elevated.

values at the base of the section and increases from 9.4 Ma, reaching maximum values prior to 8.5 Ma (Fig. 2). The values then decrease to an intermediate level at 8.5 Ma, before recovering to close to the maximum towards the top of the section (Fig. 2). The Al-MAR has distinct peaks at e.g. 9.1 Ma, 8.9 Ma and 8.75 Ma corresponding to minimum $CaCO_3$ values (Fig. 2). However, the highest Al spike at 8.65 Ma is not accompanied by a $CaCO_3$ low.

The $CaCO_3$ content in Monte Gibliscemi largely mirrors the Al-MAR. High values at the base of 40–50% decrease to minimum values of ~30% between 9.1 and 8.75 Ma (Fig. 2). Then the values increase again to ~50%, although values drop to ~30% between 8 and 7.9 Ma.

Except for isolated peaks, the Ti/Al ratio at Monte Gibliscemi does not show any major variations or trends. From the base to 9.5 Ma, the values of the ratio are distinctly lower than 0.05. In younger levels they vary around 0.05 to the top of the section (Fig. 2).

Si/Al values at Monte Gibliscemi fluctuate around 2.3 prior to 8.4 Ma, without major variations (Fig. 2). A first peak with values up to 2.45 is observed in the time interval 8.4–8.2 Ma, followed by a second peak with values of 2.6–2.8 from 8.05–7.75 Ma (Fig. 2). Then the values drop again to 2.2 which is the lowest in the section and increase to 2.6 just prior to the hiatus at 7.52 Ma (Fig. 2). In the interval of the second peak, there is a prominent drop in values at 7.9 Ma, which coincides with a diatomite layer in the section (Sprovieri et al., 1999). The Mg/Al ratio in Monte Gibliscemi shows a similar pattern to the Si/Al ratio. Relatively constant values, fluctuating around 0.25, are present prior to 8.4 Ma (Fig. 2). The Mg/Al ratio has elevated values between 8.4 and 8.25 Ma and the double peak described in the Si/Al ratio between 8.05 and 7.75 Ma is also present, with values of ~0.4. The ratio also drops at 7.9 Ma (Fig. 2) where the diatomite layer is present. After 7.75 Ma, low Si/Al values of ~0.2 return.

Prior to 8.4 Ma, there is very little variation in the Mn/Al and V/Al ratios (Fig. 3). Only Fe/Al shows isolated peaks at 9.25 and 9.1 Ma (Fig. 3) that can be associated to the presence of Fe-rich minerals. Between 8.4 and 8.2 Ma peaks are present in the Mn/Al and Fe/Al profiles which are nearly synchronous (Fig. 2). Coincident peaks in V/Al and Fe/Al are also present between 8.1 and 8 Ma, when Mn/Al does not show much variation (Fig. 3).

3.2. XRD data

The X-ray diffraction analysis shows that the Monte Gibliscemi sediments consist of a mixture of calcite, quartz, clay minerals, feldspars and traces of other minerals such as pyrite and opal (cf. Table 1). The $CaCO_3$ content is between 30 and 44%, with just one sample containing only 20%, and is therefore within the range of calculated $CaCO_3$ from the XRF data (Fig. 2). Quartz fluctuates between 11 and 18%, and the sum of the clay minerals between 37 and 50%. One sample with the lowest $CaCO_3$ has a higher clay content of 61%. The clay mineralogy is mainly kaolinite, illite, smectite, palygorskite and chlorite, moreover traces of clinoptilolite are identified in some samples and sepiolite is present in one sample (Table 1).

Of particular interest to this study are the amounts of the clay minerals kaolinite, palygorskite and sepiolite. Kaolinite is present in all samples and varies around ~20% in the clay mineral fraction. Palygorskite is not present in all samples, however, it is a component of the samples from at least 8.3 Ma onwards and then ranges between 12 and 19%. The clay mineralogical fraction of the sample at 6.95 Ma has a palygorskite content of ~35%. Sepiolite is present in a sample at 7.1 Ma.

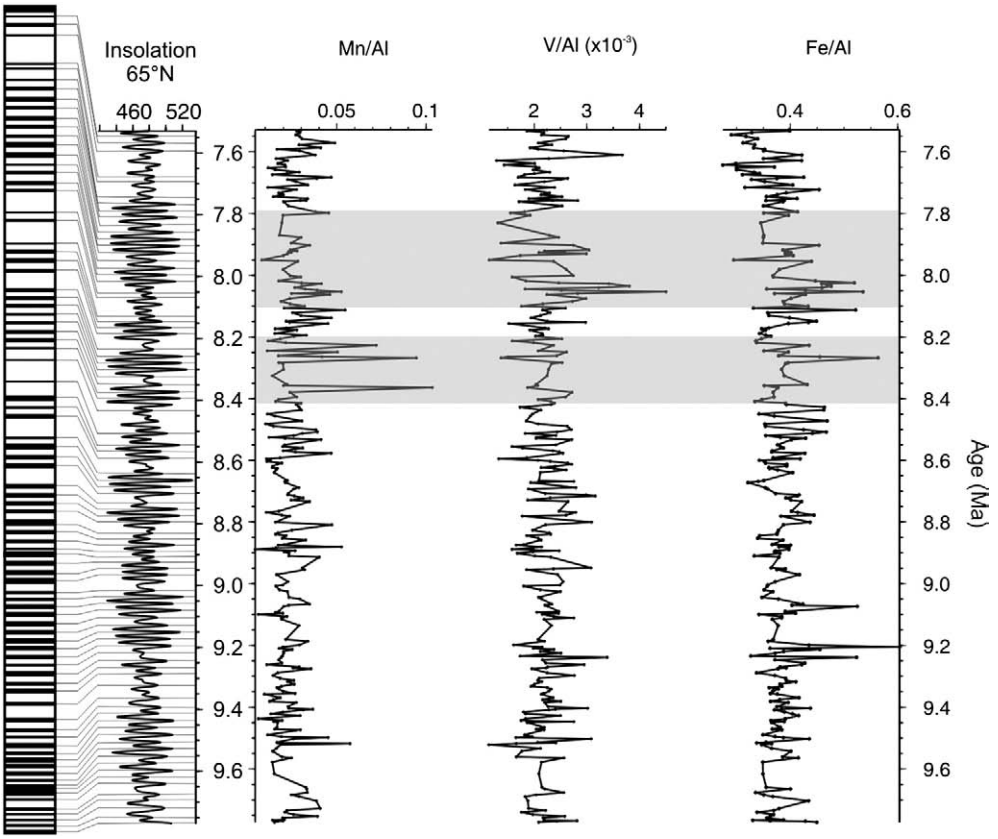

Fig. 3. Monte Gibliscemi section. Age profiles, below the hiatus; of the productivity proxies discussed in the text, below the hiatus, and a stratigraphic column to show the marl–sapropel pattern of the Monte Gibliscemi section. For an explanation of the colour coding see Fig. 2.

4. Discussion

4.1. Late Miocene climate of North Africa

The geochemical proxy records of the lower part (9.5-8.4 Ma) of the Monte Gibliscemi section show little variation, suggesting stable climatic conditions (Fig. 2). The sedimentation rate is high and the relatively low $CaCO_3$ content indicates high terrigenous input originating from the North African margin. $CaCO_3$ was calculated from Ca, assuming that 98% of the Ca resides within $CaCO_3$, providing a proxy representing marine biogenic input. Marl sediments are associated with higher $CaCO_3$ content than sapropels; Eastern Mediterranean marls have typical $CaCO_3$ concentrations around 50% (van Os et al., 1994; Wehausen and Brumsack, 1998). Sapropels are formed under more humid conditions with higher fluvial input and generally contain 20–30% $CaCO_3$ (van Os et al., 1994).

The $CaCO_3$ concentrations are low for marl intervals, but still fall within the ranges of Pleistocene carbonate cycles described by van Os et al. (1994) and are above the reported values of sapropels (25–30%) in their study. Low $CaCO_3$ values can be explained by dilution effects from high terrigenous sediment supply or by changes in palaeoproductivity (van Os et al., 1994) as carbonate dissolution is unlikely to have occurred at the depositional depth of ~1200 m. During the Pleistocene, marl deposition is associated with arid North African climatic conditions characterised by lower riverine run-off and enhanced aeolian dust production (Larrasoaña et al., 2003a).

Fluctuations in Ti/Al reflect variations in the relative importance of fluvial and aeolian transport mechanisms as Ti is associated with aeolian dust while Al is found in both aeolian and fluvial materials (Lourens et al., 2001). In Eastern Mediterranean marine sediments higher values of Ti/Al (~0.065) therefore indicate a terrigenous input dominated by aeolian dust, whilst lower ratios (~0.055) signify fluvial transport (Wehausen and Brumsack, 2000; Lourens et al., 2001; Larrasoaña et al., 2003a). The low Ti/Al ratios, around ~0.05 (Fig. 2) are in the range of what is expected of fluvial sediment supply (Nijenhuis, 1999). Values below 0.05 are the lower end member of Ti/Al ratios for modern rivers (Nijenhuis, 1999). In some intervals (8.8–8.6 Ma, 8.2–8 Ma) (Fig. 2), the ratio is ~0.06 or higher, which is closer to the values of aeolian dust ratios in the central Mediterranean (Nijenhuis, 1999; Wehausen and Brumsack, 2000). Hence it is possible that these intervals represent a relative increase in aeolian dust input. The Ti/Al ratio from Monte Gibliscemi thus indicates that North African rivers were draining into the Central Mediterranean during

Table 1
XRD derived abundances of minerals of the bulk sediment of the Monte Gibliscemi section. The clay mineralogy is calculated from the sum of the phyllosilicate fraction of the bulk Monte Gibliscemi sediment.

Section	Monte Gibliscemi						
Sub-section	GIA	GIA	GIB	GIB	GIB	GIB	GIB
Sample	25	103[a,b]	218[b,c]	62[a,c]	58	26[a,b,c]	1
Age (Ma)	9.676	9.262	8.317	7.533	7.228	7.081	6.964
$CaCO_3$ (%)	44	20	38	31	37	33	30
Quartz (%)	12	18	16	15	13	13	18
Sum of clay minerals (%)	35	61	42	50	37	49	37
Other mineral components (%)[d]	9	1	4	4	13	5	15
Kaolinite (%)[e]	31	22	21	22	19	14	27
Palygorskite (%)[e]	0	0	12	18	19	18	35
Sepiolite (%)[e]	0	0	0	0	0	22	0

[a] Traces of clinoptilolite.
[b] Traces of pyrite.
[c] Traces of opal.
[d] Includes feldspars and minor components.
[e] Calculated from total phyllosilicate amount.

the Tortonian, likely the Gabes (Fig. 1), which would imply humid conditions from at least ~9.5 Ma in northwest Africa.

The humid conditions recorded at Monte Gibliscemi during the late Tortonian do not concur with the previous results from the Metochia section of the Eastern Mediterranean (Köhler et al., 2008). On Gavdos, aeolian dust input was identified prior to ~8.2 Ma and more humid conditions thereafter (Köhler et al., 2008). Other studies have also recorded a late Miocene reduction in the dust flux off the West and East coasts of Africa (Ruddiman et al., 1989; deMenocal and Bloemendal, 1995), in particular a long record from the West coast suggests a climatic change towards more humid conditions in Central and North Africa prior to ~8 Ma (Ruddiman et al., 1989). Stable warm and humid conditions in northwest Africa, following a short interval of pronounced aridity, have been related to changes in global climate during the early late Miocene (van Zinderen Bakker and Mercer, 1986). It is therefore possible that the Monte Gibliscemi area was influenced by more humid palaeoenvironmental conditions in northwest Africa, which may have occurred earlier than the changes reported in northeast Africa (Griffin, 1999).

During the latest Tortonian, several North Africa river systems drained towards the central Mediterranean (Burke and Wells, 1989; Griffin, 2002; Griffin, 2006; Gladstone et al., 2007). In order for these rivers to flow, at least seasonally, the North African climate must be more humid than today's climate and the intertropical convergence zone (ITCZ) must have been located northward of its modern-day position, (Fluteau et al., 1999; Gladstone et al., 2007). The ITCZ must cross the central Saharan watershed of ~21°N (Rohling et al., 2002; Larrasoaña et al., 2003a) to enable rivers other than the Nile to drain into the Mediterranean (Rohling et al., 2002; Larrasoaña et al., 2003a; Griffin, 2006). The River Nile, commonly considered as an indicator of African monsoon variability, is not necessarily representative of North African climate. Its catchment area extends into (sub)-tropical regions (e.g. Rohling et al., 2002), where the Ethiopian highland experienced a late Miocene uplift phase (Gani et al., 2007) and rainfalls fed the Sudd region in Sudan (Said, 1993; Griffin, 2002).

Modelling studies show that the freshwater input from the North African rivers into the Mediterranean was threefold higher during the late Miocene than today (Gladstone et al., 2007), influencing the Eastern Mediterranean hydrological budget (Griffin, 2006). The Ti/Al ratio at Monte Gibliscemi indicates fluvial input from at least 9.5 Ma, and the locations of the North African rivers indicate late Miocene drainage of at least one of the systems into the westernmost tip of the Eastern Mediterranean (Fig. 1).

Variations in the Si/Al ratio can reflect a terrigenous North African component or changes in the amount of biosiliceous material. When interpreted to be due to a North African provenance, Si is associated with quartz and Al with detrital clays, both terrigenous components of the sediments (John et al., 2003). Their ratio is expected to remain constant unless the source area of the dust or riverine material changes. An alternative scenario to change the Si/Al ratio is to associate Si with biosiliceous activity. A choice between the two options can be made when the Mg/Al ratio is taken into consideration as well. Mg is incorporated in clay minerals, secondary carbonates and sea salts (Wehausen and Brumsack, 1998). Increases in Si/Al and Mg/Al ratios indicate a higher Si and Mg accumulation on the condition that Al flux has remained constant. Constant values of Si/Al and Mg/Al suggest an unchanging North African source area throughout the period of interest. A change in the source area of dust production could enhance the Si and Mg input relative to the clay fraction of the dust. However, the other terrigenous proxies, especially Fe/Al do not show a similar increase as Si/Al and Mg/Al (Figs. 2 and 3). Therefore it is unlikely that dust from a different region was carried to the central Mediterranean. Increasing Si/Al and Mg/Al ratios therefore either result from enhanced terrigenous supply of Si- and Mg-rich material or from changes related to restriction phases when biosiliceous productivity can be enhanced (Rouchy et al., 1995; Suc et al., 1995; Bellanca et al., 2001). Preferred conditions for biosiliceous productivity are commonly related to riverine input (Van der Zwaan, 1979; van der Zwaan, 1982) or upwelling conditions (McKenzie et al., 1979-1980) Sprovieri et al. (2008) show that $(Ba/Ca)_{carb}$ is high during the late Tortonian and associate it with increased riverine input in the central Mediterranean. This is in accordance with the modelling studies of Gladstone et al. (2007). Therefore the conditions resulting in increased biosiliceous activity likely result from increased riverine input. Interestingly, unstable run-off conditions are inferred between 8.5 and 7.5 Ma (Sprovieri et al., 2008), it is therefore possible that the run-off was high in pulses leading to the increased Si/Al and Mg/Al ratios related to the presence of biosiliceous organisms in the high productivity environment. This indicates that high values of the Si/Al ratio do not necessarily reflect the presence of diatomites but rather

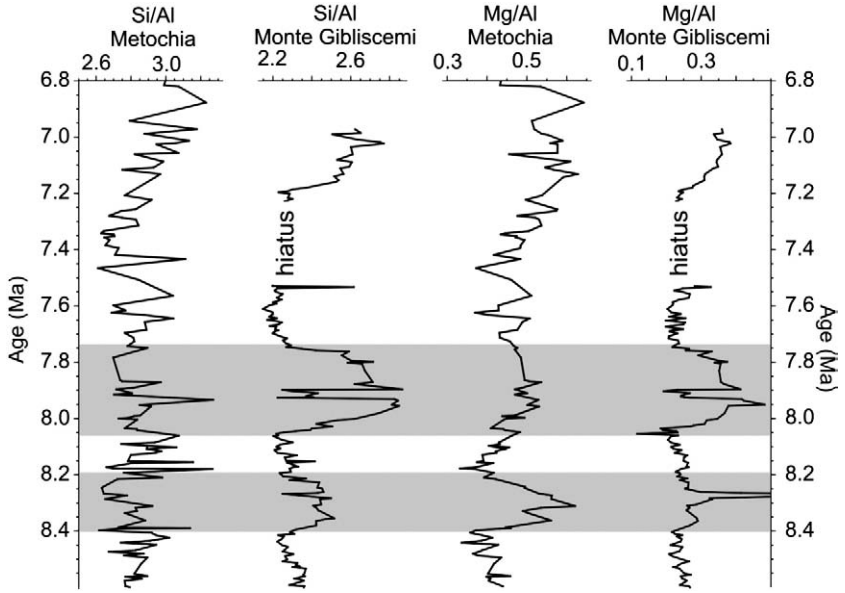

Fig. 4. Si/Al and Mg/Al ratios from the Metochia section (Köhler et al., 2008), Gavdos, compared to those from Monte Gibliscemi, extended to the time period after 7.16 Ma (early Messinian) when restrictive conditions commenced in the Mediterranean as a result of changes in the Mediterranean–Atlantic connection. The base of the Tripoli Formation on Sicily is at 7.005 Ma (Hilgen and Krijgsman, 1999).

trace high biosiliceous productivity, which then can result in the formation of diatomites.

4.2. Late Tortonian restriction of the Mediterranean

The geochemical data from Monte Gibliscemi show two large peaks in Si/Al and Mg/Al between ~8.4 and 7.8 Ma; both ratios also increase prior to the hiatus at 7.52–7.24 Ma (Fig. 2). As this hiatus is a post-depositional shear plane, these changes are not associated with it. The Si/Al and Mg/Al ratios also increase above the hiatus during the Messinian (Fig. 4). In a recent study by Köhler et al. (2008), the Miocene marls of the Metochia section of Gavdos Island, situated south of Crete were chemically analysed. This section also covers the time interval corresponding to the hiatus of the Monte Gibliscemi section (Fig. 4). Interestingly, when comparing the Si/Al and Mg/Al ratios of both sections (Fig. 4), only the Mg/Al ratio shows a broadly similar variation from 8.4 Ma onward. The Si/Al ratio just increases from 7.25 Ma onward (Fig. 4). If high Si/Al is associated with biosiliceous productivity resulting from enhanced riverine input, it would indicate that the Gavdos Basin (Metochia Section) was less influenced by riverine input. This scenario is possible as most North African rivers drained into the Eastern Mediterranean further west, i.e. closer to Monte Gibliscemi (Fig. 1). Increased fluvial input from North Africa can provide the nutrients needed for the enhanced biosiliceous productivity. However, the Ti/Al ratio tracking variation in the aeolian dust vs. riverine input does not show major changes (Fig. 2) over the time interval of interest. Therefore, it is unlikely that riverine input changed considerably from the conditions prior to the increase of biosiliceous productivity. Hence conditions not related to African climatic change appear to be the likely cause of the increase in Si and Mg.

Changes in bottom-water ventilation and productivity are traced by the Mn/Al, V/Al and Fe/Al ratios (van Santvoort et al., 1997). These ratios help identify disruptions in the Atlantic–Mediterranean connection, which can result in stagnant bottom-water conditions (van Santvoort et al., 1997; Larrasoaña et al., 2003b). Furthermore, the ratios can identify diagenetic imprints of sapropels on the marl beds. Both Mn and Fe, are remobilised and reprecipitated as a result of the downward movement of the oxidation zone during early diagenesis (van Santvoort et al., 1997). Higher V concentrations indicate reduced bottom-water ventilation (van Santvoort et al., 1997; Wehausen and Brumsack, 2000; Larrasoaña et al., 2003b). Enhanced Mn/Al, V/Al and Fe/Al ratios can also be indicative of increased biosiliceous activity when associated with enhanced silica contents in bottom water (Nijenhuis, 1999) and when Fe is not a terrigenous tracer.

The two phases of enhanced Si/Al and Mg/Al coincide with peaks in either V/Al, Mn/Al or Fe/Al at the beginning of each Si/Al and Mg/Al 'pulse' (Figs 2 and 3). The peaks of V/Al and Mn/Al are indicative of less oxygenated bottom-water conditions (Kouwenhoven et al., 1999; Larrasoaña et al., 2003b), whereas the higher Fe abundances under such conditions can be ascribed to the presence of pyrite (van Os et al., 1994). Diagenetic enrichment of Fe resulting from burnt down sapropels is unlikely as there are no related Mn enrichments at these peaks (Fig. 3). However, volcanic ash layers are known from the lower Tortonian of Sicily and can result in Fe enrichment (Kuiper et al., 2005). The proxy parameters show that isolated intervals have to be treated with care as remobilisation and diagenetic overprinting may be present in the marls. Under the assumption of stable Al fluxes this suggests restricted bottom-water circulation during this time period. Similar conditions were present at 7.6 Ma prior to the hiatus, when both the V/Al and Fe/Al ratios show a coeval peak. The first appearance of peaks in the redox sensitive ratios is synchronous with changes in Si/Al and Mg/Al (Fig. 3), suggesting that there may be a possible link between them. In present-day hypersaline anoxic basins in the Mediterranean, decreased oxygenated bottom water and increased salinity have been reported, along with an increased silica concentration of bottom waters (de Lange et al., 1990; Nijenhuis, 1999). Similar conditions have been described during oceanic convergence stages in the Neo-Tethys (Shoval, 2004), when high silica concentration conditions, combined with hypersaline bottom waters, caused authigenic formation of Mg-rich clays like palygorskite and sepiolite (Shoval, 2004).

Kaolinite is a detrital mineral commonly associated with humid conditions in North Africa (John et al., 2003) and palygorskite, when of detrital origin, reflects aridity (Chamley, 1989). Kaolinite is the prominent clay mineral present in the marls (Table 1), indicating humid palaeoenvironmental conditions in North Africa as is also indicated by the XRF elemental chemistry data. From approximately 8.3 Ma onward, palygorskite is found along with kaolinite. As both minerals are known proxies for different palaeoenvironmental conditions, it is unlikely that they have a common source area, however the Ti/Al ratio suggests humid climate. Therefore, the presence of palygorskite can be explained by either reworking of sediment or by neoformation by precipitation in the basin under Si- and Mg-rich bottom-water conditions (Singer, 1979). The sediments show traces of opal and clinoptilolite present in the bulk sediment and one sample of the Gibliscemi section has a notable sepiolite content (Table 1). Clinoptilolite can form in high productivity environments, requiring the presence of biosiliceous material (e.g. John et al., 2003). It is therefore possible that the conditions needed for authigenic clay formation were present in the elevated Si/Al zones.

Early Messinian sediments of the Mediterranean (Tripoli formation of Sicily) are also characterised by increased biosiliceous sedimentation and hypersaline conditions (Suc et al., 1995; Bellanca et al., 2001; Rouchy et al., 2001; Blanc-Valleron et al., 2002). During the early Messinian interval, the Si/Al and Mg/Al ratios of the Monte Gibliscemi section (Fig. 4) show similar values as in the earlier two intervals of elevated ratios between 8.4 and 7.8 Ma (Figs 2 and 3), suggesting similar palaeoconditions. Increased biosiliceous production in Messinian times has commonly been associated with restriction phases of the Mediterranean (e.g. Bellanca et al., 2001), because the Mediterranean–Atlantic connection through southern Morocco rapidly deteriorated at 7.1 Ma (Krijgsman et al., 1999). Therefore, increases in the Si/Al ratio are taken as a first approximation for restrictive phases present in the record. Restrictive phases have previously been identified in the foraminifera record of Monte Gibliscemi at 8.5 Ma and 8 Ma, with benthic foraminifera diversities changing towards more stress tolerant species (Kouwenhoven et al., 1999; Seidenkrantz et al., 2000). These changes in the late Miocene Mediterranean sediments were linked to Mediterranean–Atlantic gateway dynamics (Hüsing et al., 2009).

During the late Miocene, the Mediterranean was connected to the Atlantic ocean via two gateways: the Rifian corridor (Morocco) (Krijgsman et al., 1999) and the Betics (southern Spain) (Soria et al., 1999). These connections became gradually restricted, causing the Mediterranean to become more isolated, finally resulting in the Messinian Salinity Crisis (Hsü et al., 1973). The first connection that closed was the North Betic gateway through southern Spain during the early Tortonian (Martin et al., 2009), followed by the Guadix and Granada basins in the late Tortonian (Soria et al., 1999; Betzler et al., 2006). New magneto-biostratigraphic results from the Guadix basin, which has a central position in the gateway, indicates that a significant hiatus, comprising the latest Tortonian and early Messinian, is present in the sedimentary successions, suggesting that the gateway may have been open during the Messinian (Hüsing et al., 2009; Hüsing et al., under review). Magnetostratigraphic dating of the sedimentary sequences of the Lorca and Fortuna basins in the east part of the gateway, indicated that open marine sedimentation ceased entirely at ~7.8 Ma, culminating in the deposition of diatomites and evaporites of the Tortonian salinity crisis of the eastern Betics (Krijgsman et al., 2000). As a result of these conditions the circulation in the Mediterranean may have become more sluggish causing water body stratification, increasing oxygen stress and bottom-water salinity (Kouwenhoven et al., 1999; Seidenkrantz et al., 2000; Kouwenhoven et al., 2003) and the formation of anoxic basins

(Kouwenhoven and van der Zwaan, 2006). To drive such weak circulation supporting the formation of biosiliceous sediment and authigenic clays, the connections of the Mediterranean Sea and the Atlantic Ocean must be deep enough to allow water exchange (Meijer et al., 2004). However, the depth of the Sicilian sill, which forms the boundary between the Western and Eastern Mediterranean basins is important and cannot be neglected. Its depth is important in controlling circulation in the Eastern basin (Meijer et al., 2004). The circulation in the Eastern Mediterranean is further influenced by the salinity in the Adriatic Basin, where lower salinities, caused by higher influx of Atlantic water (deeper sill) reduce the dense deep water (Meijer et al., 2004). As a result, the deep circulation of the Eastern Mediterranean decreases (Meijer et al., 2004).

The sudden termination of the Si/Al and Mg/Al peaks at ~7.8 Ma suggests that restricted conditions in the Mediterranean also terminated rapidly, with open connections being re-established quickly. It is most likely that the Rifian Corridor caused this change, because the late Miocene sedimentary records of the Rifian foredeep show a significant marine transgression during the late Tortonian which has been interpreted as the opening of the Rifian Corridor (Krijgsman et al., 1999). Magneto-biostratigraphic age constraints on this transgression event (between 8 and 7.6 Ma) were extrapolated from the base of the Zobzit section in the Taza–Guercif basin and are not very accurate. Our results from Monte Gibliscemi suggest that it occurred at 7.8 Ma.

5. Conclusions

The sedimentary archive of Monte Gibliscemi provides a late Miocene record of North African palaeoenvironmental conditions and disruptions in the Mediterranean–Atlantic connection. North Africa was humid with rivers draining into the central Mediterranean, and fluvial input dominating over aeolian contributions from 9.5 Ma throughout the section. There are two phases between 8.4 and 7.8 Ma, when the geochemistry of the marls is similar to early Messinian sediments with enhanced biosiliceous sedimentation, interpreted to result from weaker circulation in the Eastern Mediterranean. These conditions enabled the formation of authigenic palygorskite in the basin and are linked to disruptions of the Mediterranean–Atlantic connections, which changed gradually from the late Tortonian. Our data suggests that the transgression associated with the opening of the Rifian corridor occurred at 7.8 Ma.

Acknowledgements

This study was financed by the DFG International Graduate College EUROPROX. Paul Th. Meijer is thanked for carefully reading the manuscript and his useful comments. We are thankful for helpful discussions with S. Hüsing. We also thank K. Enneking for the laboratory assistance and C. Vogt for XRD measurements. Three anonymous reviewers are thanked for their constructive reviews.

References

Bellanca, A., Caruso, A., Ferruzza, G., Rouchy, J.M., Sprovieri, M., Blanc-Valleron, M.M., 2001. Transition from marine to hypersaline conditions in the Messinian Tripoli Formation from the marginal areas of the central Sicilian Basins. Sedimentary Geology 140, 87–105.

Benson, R.H., Rakic-El Bied, K., Bonaduce, G., 1991. An important current reversal (influx) in the Rifian Corridor (Morocco) at the Tortonian–Messinian boundary: the end of the Tethys Ocean. Paleoceanography 6, 164–192.

Bergametti, G., Gomes, L., Coude-Gaussen, G., Rognon, P., Le Coustumer, M.-N., 1989. African dust observed over Canary Islands: source-regions identification and transport pattern for some summer situations. Journal of Geophysical Research 94, 14855–14864.

Betzler, C., Braga, J.C., Martin, J.M.M., Sánchez-Almazo, I.M., Lindhorst, S., 2006. Closure of a seaway: stratigraphic record and facies (Guadix Basin, Southern Spain). International Journal of Earth Sciences 95, 903–910.

Blanc-Valleron, M.-M., Pierre, C., Caulet, J.P., Caruso, A., Rouchy, J.-M., Cespuglio, G., Sprovieri, R., Pestrea, S., Di Stefano, E., 2002. Sedimentary, stable isotope and micropaleontological records of paleoceanographic change in the Messinian Tripoli Formation (Sicily, Italy). Palaeogeography, Palaeoclimatology, Palaeoecology 185, 255–286.

Burke, K., Wells, G.L., 1989. Trans-African drainage system of the Sahara: was it the Nile? Geology 17, 743–747.

Chamley, H., 1989. Clay Mineralogy. Springer-Verlag, Berlin. 623 pp.

de Lange, G.J., Boelrijk, N.A.I.M., Catalano, G., Corselli, C., Klinkhammer, G.P., Middelburg, J.J., Müller, D.W., Ullman, W.J., van Gaans, P., Woittiez, J.R.W., 1990. Sulphate-related equilibria in the hypersaline brines of the Tyro and Bannock Basins, eastern Mediterranean. Marine Chemistry 31, 89–112.

deMenocal, P.B., Bloemendal, J., 1995. Plio–Pleistocene variability in subtropical Africa and the paleoenvironment of Hominid evolution: a combined data-model approach. Paleoclimate and Evolution with Emphasis on Human Origins. Yale University Press, New Haven & London, pp. 389–407.

Flecker, R., de Villiers, S., Ellam, R.M., 2002. Modelling the effect of evaporation on the salinity — $^{87}Sr/^{86}Sr$ relationship in modern and ancient marginal–marine system: the Mediterranean Messinian Salinity Crisis. Earth and Planetary Science Letters 203, 221–233.

Fluteau, F., Ramstein, G., Besse, J., 1999. Simulating the evolution of the Asian and African monsoons during the past 30 Myr using an atmospheric general circulation model. Journal of Geophysical Research 104 (D10), 11995–12018.

Gani, N.D.S., Gani, M.R., Abdelsalam, M.G., 2007. Blue Nile incision on the Ethiopian Plateau: pulsed plateau growth, Pliocene uplift, and hominin evolution. GSA Today 17 (9), 4–11.

Gladstone, R., Flecker, R., Valdes, P., Lunt, D., Markwick, P., 2007. The Mediterranean hydrological budget from a Late Miocene global climate simulation. Palaeogeography, Palaeoclimatology, Palaeoecology 251, 254–267.

Griffin, D.L., 1999. The late Miocene climate of northeastern Africa: unravelling the signals in the sedimentary succession. Journal of the Geological Society 156, 817–826.

Griffin, D.L., 2002. Aridity and humidity: two aspects of late Miocene climate of North Africa and the Mediterranean. Palaeogeography, Palaeoclimatology, Palaeoecology 182, 65–91.

Griffin, D.L., 2006. The late Neogene Sahabi rivers of the Sahara and their climatic and environmental implications for the Chad Basin. Journal of the Geological Society 163, 905–921.

Hilgen, F.J., Krijgsman, W., 1999. Cyclostratigraohy and astrochronology of the Tripoli diatomite formation (pre-evaporite Messinian, Sicily, Italy). Terra Nova 11, 16–22.

Hilgen, F.J., Krijgsman, W., Langereis, C.G., Lourens, L.J., Santarelli, A., Zachariasse, W.J., 1995. Extending the astronomical (polarity) time scale into the Miocene. Earth and Planetary Science Letters 136, 495–510.

Hsü, K.J., Ryan, W.B.F., Cita, M.B., 1973. Late Miocene desiccation of the Mediterranean. Nature 242, 240–244.

Hüsing, S.K., Dekkers, M.J., Franke, C., Krijgsman, W., 2009. The Tortonian reference section at Monte dei Corvi (Italy): evidence for early remanence acquisition in greigite-bearing sediments. Geophysical Journal International 179, 125–143.

Hüsing, S.K., Oms, O., Agustí, J., Garcés, M., Kouwenhoven, T.J., Krijgsman, W., Zachariasse, W.J., under review. On the late Miocene closure of the Mediterranean–Atlantic gateway through the Guadix Basin (southern Spain). Palaeogeography Palaeoclimatology Palaeoecology.

John, C.M., Mutti, M., Adatte, T., 2003. Mixed carbonate–siliciclastic record on the North African margin (Malta) — coupling of weathering processes and mid-Miocene climate. GSA Bulletin 115 (2), 217–229.

Köhler, C.M., Heslop, D., Dekkers, M.J., Krijgsman, W., van Hinsbergen, D.J.J., von Dobeneck, T., 2008. Tracking provenance changes during the late Miocene in the Eastern Mediterranean Metochia section using geochemical and environmental magnetic proxies. Geochemistry, Geophysics, Geosystems 9, Q12018. doi:10.1029/2008GC002127.

Köhler, C.M., Krijgsman, W., Van Hinsbergen, D.J.J., Heslop, D., in press. Concurrent tectonic and climatic changes recorded in upper Tortonian sediments from the Eastern Mediterranean. Terra Nova.

Kouwenhoven, T.J., Seidenkrantz, M.-S., van der Zwaan, G.J., 1999. Deep-water changes: the near-synchronous disappearance of a group of benthic foraminifera from the Late Miocene Mediterranean. Palaeogeography, Palaeoclimatology, Palaeoecology 152, 259–281.

Kouwenhoven, T.J., Hilgen, F.J., van der Zwaan, G.J., 2003. Late Tortonian–early Messinian stepwise disruption of the Mediterranean Atlantic connections: constraints from benthic foraminiferal and geochemical data. Palaeogeography, Palaeoclimatology, Palaeoecology 198, 303–319.

Kouwenhoven, T.J., van der Zwaan, G.J., 2006. A reconstruction of late Miocene Mediterranean circulation patterns using benthic foraminifera. Palaeogeography, Palaeoclimatology, Palaeoecology 238, 373–385.

Krijgsman, W., Hilgen, F.J., Langereis, C.G., Santarelli, A., Zachariasse, W.J., 1995. Late Miocene magnetostratigraphy, biostratigraphy and cyclostratigraphy in the Mediterranean. Earth and Planetary Science Letters 136, 475–494.

Krijgsman, W., Langereis, C.G., Zachariasse, W.J., Boccaletti, M., Moratti, G., Gelati, R., Iaccarino, S., Papani, G., Villa, G., 1999. Late Neogene evolution of the Taza–Guercif Basin (Rifian Corridor, Morocco) and implications for the Messinian salinity crisis. Marine Geology 153, 147–160.

Krijgsman, W., Garcés, M., Agustí, J., Raffi, I., Taberner, C., Zachariasse, W.J., 2000. The 'Tortonian Salinity Crisis' of the Eastern Betics. Earth and Planetary Science Letters 181, 497–511.

Kuiper, K.F., Wijbrans, J.R., Hilgen, F.J., 2005. Radioisotopic dating of the Tortonian Global Stratotype Section and Point: implications for intercalibration of $^{40}Ar/^{39}Ar$ and astronomical dating methods. Terra Nova 17, 385–398.

Larrasoaña, J.C., Roberts, A.P., Rohling, E.J., Winklhofer, M., Wehausen, R., 2003a. Three million years of monsoon variability over the northern Sahara. Climate Dynamics 21, 689–698.

Larrasoaña, J.C., Roberts, A.P., Stoner, J.S., Richter, C., Wehausen, R., 2003b. A new proxy for bottom-water ventilation in the eastern Mediterranean based on diagentically controlled magnetic properties of sapropel-bearing sediments. Palaeogeography, Palaeoclimatology, Palaeoecology 190, 221–242.
Laskar, J., Robutel, P., Joutel, F., Gastineau, M., Correia, A.C.M., Levard, B., 2004. A long-term numerical solution for the insolation quantities of the Earth. Astronomy & Astrophysics 428, 261–285.
Lihoreau, F., Boisserie, J.-R., Viriot, L., Coppens, Y., Likius, A., MacKaye, H.T., Tafforeau, P., Vignaud, P., Brunet, M., 2006. Anthracothere dental anatomy reveals a late Miocene Chado–Libyan bioprovince. PNAS 103 (23), 8763–8767.
Lourens, L.J., Wehausen, R., Brumsack, H.-J., 2001. Geological constraints on tidal dissipation and dynamical ellipticity of the Earth over the past three million years. Nature 409, 1029–1033.
Martin, J.M., Braga, J.C., Aguirre, J., Puga-Bernabeu, A., 2009. History and evolution of the North–Betic Strait (Prebetic Zone, Betic Cordillera): a narrow, early Tortonian, tidal-dominated, Atlantic–Mediterranean marine passage. Sedimentary Geology 216 (3–4), 80–90.
McKenzie, J.A., Jenkyns, H.C., Bennett, G.G., 1979–1980. Stable isotope study of the cyclic diatomite-claystones from the Tripoli formation, Sicily: a prelude to the Messinian salinity crisis. Palaeogeography, Palaeoclimatology, Palaeoecology 29, 125–142.
Meijer, P.T., Krijgsman, W., 2005. A quantitative analysis of the desiccation and re-filling of the Mediterranean during the Messinian Salinity Crisis. Earth and Planetary Science Letters 240, 510–520.
Meijer, P.T., Slingerland, R., Wortel, M.J.R., 2004. Tectonic control on past circulation of the Mediterranean Sea: a model study of the Late Miocene. Paleoceanography 19, PA 1026.
Middleton, N.J., 1985. Effects of drought on dust production in the Sahel. Nature 316, 431–434.
Nijenhuis, I.A., 1999. Geochemistry of eastern Mediterranean sedimentary cycles: on the origin of Miocene to Pleistocene sapropels, laminites and diatomites. Universiteit Utrecht, Utrecht. 167 pp.
Orszag-Sperber, F., Butterlin, J., Clermonte, J., Colchen, M., Giraud, R., Poisson, A., Ricou, L.E., 1993. Tortonian palaeoenvironments (1.5–6 Ma). In: Vrielynch, B. (Ed.), Atlas Tethys Palaeoenvironmental Maps. Cauthier Villars, Paris, pp. 243–258.
Peterson, L.C., Haug, G.H., Hughen, K.A., Röhl, U., 2000. Rapid changes in the hydrological cycle of the Tropical Atlantic during the last glacial. Science 290, 1947–1951.
Rohling, E.J., Cane, T.R., Cooke, S., Sprovieri, M., Bouloubassi, I., Emeis, K.C., Schiebel, R., Kroon, D., Jorissen, F.J., Lorre, A., Kemp, A.E.S., 2002. African monsoon variability during the previous interglacial maximum. Earth and Planetary Science Letters 202, 61–75.
Rossignol-Strick, M., Paterne, M., Bassinot, F.C., Emais, K.-C., De Langes, G.J., 1998. An unusual mid-Pleistocene monsoon period over Africa and Asia. Nature 392, 269–272.
Rouchy, J.M., Noel, D., Wali, A.M.A., Aref, M.A.M., 1995. Evaporitic and biosiliceous cyclic sedimentation in the Miocene of the Gulf of Suez — depositional and diagenetic aspects. Sedimentary Geology 94, 277–297.
Rouchy, J.M., Orszag-Sperber, F., Blanc-Valleron, M.-M., Pierre, C., Rivière, M., Combourieu-Nebout, N., Panayides, I., 2001. Paleoenvironmental changes at the Messinian–Pliocene boundary in the eastern Mediterranean (southern Cyprus basins): significance of the Messinian Lago–Mare. Sedimentary Geology 145, 93–117.
Ruddiman, W.F., Sarnthein, M., Backman, J., Baldauf, J.G., Curry, W., Dupont, L.M., Janecek, T., Pokras, E.M., Raymo, M.E., Stabell, B., Stein, R., Tiedemann, R., 1989. Late Miocene to Pleistocene evolution of climate in Africa and the low-latitude Atlantic: overview of Leg 108 results. Proceedings of the Ocean Drilling Program, Scientific Results 108, 463–484.
Said, R., 1993. The River Nile. Geology, Hydrology and Utilization. Pergamon Press, New York.
Schenau, S.J., Antonarakou, A., Hilgen, F.J., Lourens, L.J., Nijenhuis, I.A., van der Weijden, C.H., Zachariasse, W.J., 1999. Organic-rich layers in the Metochia section (Gavdos, Greece): evidence for a single mechanism of sapropel formation during the past 10 My. Marine Geology 153, 117–135.
Seidenkrantz, M.-S., Kouwenhoven, T.J., Jorissen, F.J., Shackleton, N.J., van der Zwaan, G.J., 2000. Benthic foraminifera as indicators of changing Mediterranean–Atlantic water exchange in the late Miocene. Marine Geology 2000 (163), 387–407.
Shoval, S., 2004. Clay sedimentation along the southeastern Neo-Tethys margin during the oceanic convergence stage. Applied Clay Science 24, 287–298.
Singer, A., 1979. Palygorskite in sediments: detrital, diagenetic or neoformed. A critical review. Geologische Rundschau 68, 996–1008.
Soria, J.M., Fernández, J., Viseras, C., 1999. Late Miocene stratigraphy and palaeogeographic evolution of the intramontane Guadix Basin (Central Betic Cordillera, Spain): implications for an Atlantic–Mediterranean connection. Palaeogeography, Palaeoclimatology, Palaeoecology 151, 255–266.
Sprovieri, M., Bellanca, A., Neri, R., Mazzola, S., Bonanno, A., Patti, B., Sorgente, R., 1999. Astronomical calibration of late Miocene stratigraphic events and analysis of precessionally driven paleoceanographic changes in the Mediterranean basin. Memorie della Società Geologica Italiana 54, 7–24.
Sprovieri, M., d'Alcala, M.R., Manta, D.S., Bellanca, A., Neri, R., Lirer, F., Taberner, C., Pueyo, J.J., Sammartino, S., 2008. Ba/Ca evolution in water masses of the Mediterranean late Neogene. Paleoceanography 23 (3). doi:10.1029/2007PA00246.
Suc, J.-P., Violanti, D., Londeix, L., Poumot, C., Robert, C., Clauzon, G., Gautier, F., Turon, J.-L., Ferrier, J., Chikhi, H., Cambon, G., 1995. Evolution of the Messinian Mediterranean environments: the Tripoli Formation at Capodarso (Sicily, Italy). Review of Palaeobotany and Palynology 87, 51–79.
Van der Zwaan, G.J., 1979. The pre-evaporite Late Miocene environment of the Mediterranean: stable isotopes of planktonic foraminifera from section Falconara, Sicily. Koninklijke Nederlandse Akademie van Wetenschappen 82, 487–502.
van der Zwaan, G.J., 1982. Middle Miocene–Pliocene Mediterranean foraminifera. Utrecht Micropaleontological Bulletins 10, 71–90.
van Os, B.J.H., Lourens, L.J., Hilgen, F.J., de Lange, G.J., Beaufort, L., 1994. The formation of Pliocene sapropels and carbonate cycles in the Mediterranean: diagenesis, dilution and productivity. Paleoceanography 9 (4), 601–617.
van Santvoort, P.J.M., de Lange, G.J., Langereis, C.G., Dekkers, M.J., 1997. Geochemical and paleomagnetic evidence for the occurrence of "missing" sapropels in eastern Mediterranean sediments. Paleoceanography 12 (6), 773–786.
van Zinderen Bakker, E.M., Mercer, J.H., 1986. Major late Cainozoic climatic events and palaeoenvironmental changes in Africa viewed in a world wide context. Palaeogeography, Palaeoclimatology, Palaeoecology 56, 217–235.
Vogt, C., Lauterjung, J., Fischer, R.X., 2002. Investigation of the clay fraction (2 µm) of the clay minerals society reference clays. Clays and Clay Minerals 50 (3), 388–400.
Wehausen, R., Brumsack, H.-J., 1998. The formation of Pliocene Mediterranean sapropels: constraints from high-resolution major and minor element studies. In: Robertson, A.H.F., Emeis, K.-C., Camerlenghi, A. (Eds.), Proceedings of the Ocean Drilling Program, Scientific Results. Ocean Drilling Program, College Station, Texas, pp. 207–217.
Wehausen, R., Brumsack, H.-J., 2000. Chemical cycles in Pliocene sapropel-bearing and sapropel barren eastern Mediterranean sediments. Palaeogeography, Palaeoclimatology, Palaeoecology 158, 325–352.